⌘ *Author's Choice*

THE JOURNAL OF BIOLOGICAL CHEMISTRY VOL. 287, NO. 9, pp. 6128–6138, February 24, 2012

Amplification and Demultiplexing in Insulin-regulated Akt Protein Kinase Pathway in Adipocytes*[S]

Received for publication, October 28, 2011, and in revised form, December 26, 2011 Published, JBC Papers in Press, December 29, 2011, DOI 10.1074/jbc.M111.318238

Shi-Xiong Tan[‡], Yvonne Ng[‡], Christopher C. Meoli[‡], Ansu Kumar[§], Poh-Sim Khoo[¶], Daniel J. Fazakerley[‡1], Jagath R. Junutula[¶], Shireen Vali[§], David E. James[‡‖2], and Jacqueline Stöckli[‡]

From the [‡]Diabetes and Obesity Research Program, The Garvan Institute of Medical Research, 384 Victoria Street, Darlinghurst, Sydney, New South Wales 2010, Australia, the [‖]School of Biotechnology and Biomolecular Sciences, University of New South Wales, Sydney, New South Wales 2050, Australia, [§]Cellworks Group, Inc., Saratoga, California 95070, and [¶]Genentech, Inc., South San Francisco, California 94080

Background: Akt plays a major role in insulin regulation of metabolism.
Results: Akt operates at 5–22% of its dynamic range. This lacks concordance with Akt substrate phosphorylation, GLUT4 translocation, and protein synthesis.
Conclusion: Akt is a demultiplexer that splits the insulin signal into discrete outputs.
Significance: This study provides better understanding of the Akt pathway and has implications for the role of Akt in diseases.

Akt plays a major role in insulin regulation of metabolism in muscle, fat, and liver. Here, we show that in 3T3-L1 adipocytes, Akt operates optimally over a limited dynamic range. This indicates that Akt is a highly sensitive amplification step in the pathway. With robust insulin stimulation, substantial changes in Akt phosphorylation using either pharmacologic or genetic manipulations had relatively little effect on Akt activity. By integrating these data we observed that half-maximal Akt activity was achieved at a threshold level of Akt phosphorylation corresponding to 5–22% of its full dynamic range. This behavior was also associated with lack of concordance or demultiplexing in the behavior of downstream components. Most notably, FoxO1 phosphorylation was more sensitive to insulin and did not exhibit a change in its rate of phosphorylation between 1 and 100 nM insulin compared with other substrates (AS160, TSC2, GSK3). Similar differences were observed between various insulin-regulated pathways such as GLUT4 translocation and protein synthesis. These data indicate that Akt itself is a major amplification switch in the insulin signaling pathway and that features of the pathway enable the insulin signal to be split or demultiplexed into discrete outputs. This has important implications for the role of this pathway in disease.

The protein kinase Akt, also known as protein kinase B (PKB), is involved in many fundamental biological processes including cell survival, proliferation, growth, and metabolism (1, 2). In insulin-responsive tissues, activation of Akt involves binding of insulin to the insulin receptor. This triggers the activation of its tyrosine kinase activity and results in its autophosphorylation and recruitment of scaffolding proteins such as IRS1.[3] Tyrosyl-phosphorylated IRS1 acts as a platform for the assembly of a signaling node comprising among other proteins the lipid kinase phosphatidylinositol 3-kinase (PI3K) leading to the generation of phosphatidylinositol 3,4,5-trisphosphate ($PI(3,4,5)P_3$). This facilitates the translocation of Akt to the plasma membrane (PM) where it is phosphorylated at Thr-308 and Ser-473 by phosphoinositide-dependent kinase 1 and the mammalian target of rapamycin (mTOR) complex 2 (mTORC2), respectively (3, 4). Upon activation, Akt phosphorylates a range of substrates such as glycogen synthase kinase 3 (GSK3), the Rab GTPase-activating protein (RabGAP) AS160, also called TBC1D4, proline-rich Akt substrate of 40 kDa (PRAS40), and RhebGAP tuberous sclerosis protein 2 (TSC2). The phosphorylation of these substrates orchestrates a complex metabolic program involving the translocation of the glucose transporter GLUT4 to the PM leading to glucose uptake into cells, increased glycogen and protein synthesis as well as long term effects on transcription (5, 6).

The PI3K/Akt pathway is often portrayed as a linear cascade whereby unitary changes in flux are transmitted equally throughout the signaling network. However, this is likely to be an oversimplification. First, insulin-responsive cells possess "spare" receptors (7) whereby occupancy of a small number of receptors is sufficient to achieve a maximal biological outcome. This situation is thought to contribute to flexibility in terms of the sensitivity and the intensity of insulin action. Second, the Akt pathway possesses a number of feedback loops that attenuate transmission of the signal again adding to the nonlinearity in this system. Most notably, mTOR as well as other downstream kinases such as S6 kinase, phosphorylate upstream elements in the Akt signaling pathway including IRS1 (8–11) or Rictor (12), and this is often correlated with reduced Akt activity. This negative feedback loop is widely considered to play an

* This work was supported by grants from the National Health and Medical Research Council of Australia.
⌘ *Author's Choice*—Final version full access.
[S] This article contains supplemental Figs. S1–S3.
[1] Sir Henry Wellcome Postdoctoral Fellow of the Wellcome Trust.
[2] National Health and Medical Research Council Senior Principal Research Fellow. To whom correspondence should be addressed. E-mail: d.james@garvan.org.au.

[3] The abbreviations used are: IRS, insulin receptor substrate; Akti, isoform-specific inhibitor of Akt; GLUT4, glucose transporter 4; GSK, glycogen synthase kinase; mTOR, mammalian target of rapamycin; $PI(3,4,5)P_3$, phosphatidylinositol 3,4,5-trisphosphate; PM, plasma membrane; PRAS40, proline-rich Akt substrate of 40 kDa; TSC2, tuberous sclerosis protein 2.

important role in the development of insulin resistance, a major pathophysiological feature of metabolic disease. Third, many of the components in this system such as Akt possess enzymatic activity and so have the intrinsic capacity for signal amplification. Fourth, several network components such as PI3K and Akt comprise multiple isoforms displaying characteristically discrete behavior (13–17). Finally, some of the network components are subject to spatial regulation (14, 18), providing further rationale for nonlinearity.

Here, we show that, as is the case for the insulin receptor, Akt also exhibits nonlinear behavior such that the relationship between Akt phosphorylation at its two major regulatory sites, and downstream kinase activity is sigmoidal. Moreover, discrete relationships between Akt phosphorylation and different metabolic actions of insulin known to be downstream of Akt were observed, suggesting that this single pathway is capable of demultiplexing and splitting the upstream insulin signal into discrete outputs. This has implications for the way that this system operates in disease.

EXPERIMENTAL PROCEDURES

Materials and Antibodies—Polyclonal rabbit antibodies pThr-308 Akt, pThr-1462 TSC2, pSer-21/9 GSK3α/β, pSer-246 PRAS40, total PRAS40, and pThr-389 p70 S6 kinase, monoclonal rabbit antibodies raised against total Akt (11E7), Akt2 (D6G4), and total GSK3β (27C10), and monoclonal mouse antibodies raised against pSer-473 Akt (587F11), Akt1 (2H10), and pTyrosines (pY100) were purchased from Cell Signaling Technologies (Beverly, MA). Polyclonal rabbit antibody raised against TSC2 and 14-3-3β was purchased from Santa Cruz Biotechnology, Inc. (Santa Cruz, CA). Polyclonal sheep antibodies raised against pSer-588 AS160 and pThr-642 AS160 were obtained from Peter Shepherd (Symansis, Auckland, New Zealand). Rabbit polyclonal antibodies against human AS160 were produced as described previously (19). Tubulin antibody was from Sigma. Monoclonal anti-HA antibody was obtained from Covance (Berkeley, CA). Horseradish peroxidase-conjugated secondary antibodies were from Amersham Biosciences, and IRDye 700- or 800-conjugated secondary antibodies were from Rockland Immunochemicals (Gilbertsville, PA). Paraformaldehyde was from ProSciTech (Thuringowa, Australia). Dulbecco's modified Eagle's medium (DMEM) and newborn calf serum were from Invitrogen. Fetal calf serum was from Trace Scientific (Melbourne, Australia), and antibiotics were from Invitrogen. Bovine serum albumin (BSA) was from Bovogen (Essendon, Australia). Bicinchoninic acid reagent and SuperSignal West Pico chemiluminescent substrate were from Pierce. Protease inhibitor mixture tablets were from Roche Applied Science. The Akt1-specific and Akt2-specific inhibitors were previously described (20) and were obtained from Merck. The Akt inhibitor, MK-2206, was generously provided by Professor Dario Alessi (University of Dundee, Dundee, UK). Other materials were obtained from Sigma.

Cell Culture—3T3-L1 fibroblasts (ATCC, Manassas, VA) were cultured and differentiated to adipocytes as described previously (21). 3T3-L1 fibroblasts were infected with either pBabepuro-HA-GLUT4 retrovirus only or together with pLXSN PDGFR retrovirus. After a 24-h recovery period, infected cells were selected with either 2 μg/ml puromycin or together with 800 μg/ml Geneticin in DMEM supplemented with 10% fetal calf serum for selection of HA-GLUT4-infected cells or HA-GLUT4/PDGFR-infected cells, respectively. Surviving 3T3-L1 fibroblasts were then grown to confluence and subsequently differentiated into adipocytes as described above.

Western Blot Analysis—Cells were washed twice with ice-cold PBS and solubilized in 2% SDS in PBS containing phosphatase inhibitors (1 mM sodium pyrophosphate, 2 mM sodium vanadate, 10 mM sodium fluoride) and complete protease inhibitor mixture. Insoluble material was removed by centrifugation at 18,000 $\times$ *g* for 10 min. Protein concentration was measured using the bicinchoninic acid method. Proteins were separated by SDS-PAGE for immunoblot analysis. After transferring proteins to polyvinylidene difluoride membranes, membranes were incubated in blocking buffer containing 5% skim milk in Tris-buffered saline and immunoblotted with the relevant antibodies overnight at 4 °C in blocking buffer containing 5% BSA, 0.1% Tween in Tris-buffered saline. After incubation, membranes were washed and incubated with horseradish peroxidase-labeled secondary antibodies and then detected by SuperSignal West Pico chemiluminescent substrate. In some cases, IRDye 700- or 800-conjugated secondary antibodies were used and then scanned at the 700 nm and 800 nm channel using the Odyssey IR imager. Quantification of protein levels was performed using Odyssey IR imaging system software or the Wright Cell Imaging Facility ImageJ software.

Immunoprecipitation—Following the indicated treatment, cells were washed with ice-cold PBS and solubilized in Nonidet P-40 buffer (50 mm Tris-HCl, pH 7.5, 150 mm NaCl, 1% Nonidet P-40, 1 mm EDTA, and 10% glycerol) containing Complete protease inhibitor mixture and phosphatase inhibitors (2 mm sodium orthovanadate, 1 mm sodium pyrophosphate, 10 mm sodium fluoride). Cell lysates were homogenized 10 times using a 27-gauge needle and centrifuged at 18,000 $\times$ *g* for 20 min at 4 °C. One mg of cell lysates was incubated overnight at 4 °C with 2 μl of monoclonal mouse Akt1 antibody, monoclonal rabbit Akt2, or nonimmunized rabbit or mouse IgG. Antibodies were then captured with protein G-Sepharose beads for 2 h at 4 °C. Immunoprecipitates were washed three times with ice-cold Nonidet P-40 buffer and kept in 2 $\times$ SDS sample buffer at −20 °C.

Quantitative GLUT4 Translocation Assay—HA-GLUT4 translocation to the PM was measured as described previously (22). Briefly, 3T3-L1 adipocytes stably expressing PDGFR and/or HA-GLUT4 in 96-well plates were serum-starved with Krebs-Ringer phosphate buffer (0.6 mM Na_2HPO_4, 0.4 mM NaH_2PO_4, 120 mM NaCl, 6 mM KCl, 1 mM $CaCl_2$, 1.2 mM $MgSO_4$, 12.5 mM HEPES, pH 7.4) supplemented with 0.2% BSA and with 20 nM rapamycin where indicated for 2 h. Cells were then treated with dimethyl sulfoxide or the indicated compound for 30 min prior to insulin stimulation for 20 min or as indicated. After stimulation, cells were fixed and immunolabeled with monoclonal anti-HA antibody followed by Alexa Fluor 488-labeled secondary antibody in the absence or presence of saponin to analyze the amount of HA-GLUT4 at the PM or the total HA-GLUT4 content, respectively.

Protein Synthesis Assay—3T3-L1 fibroblasts were seeded and differentiated into adipocytes in 24-well plates. Cells were washed twice and incubated with Krebs-Ringer phosphate buffer supplemented with 0.2% BSA for 2 h prior to insulin stimulation for 20 min. [^{3}H]Leucine (PerkinElmer Life Sciences) was added at the same time as insulin to a final concentration of 5 μCi/ml. To determine nonspecific leucine uptake, 5 μM cyclohexamide was added for 1 h before addition of [^{3}H]leucine and insulin. Leucine incorporation was terminated with three rapid washes in ice-cold PBS follow by incubating cells with 10% trichloroacetic acid (TCA) for 10 min to precipitate proteins. Pellets were washed three times in 10% TCA to remove free [^{3}H]leucine that was not incorporated. Pellets were resuspended in 50 nM NaOH with 1% Triton X-100 at 65 °C for 20 min. Samples were assessed for radioactivity by scintillation counting using the β-scintillation counter. The nonspecific uptake was subtracted, and results were normalized for protein content using BCA analysis. Each condition was performed in triplicate.

Cationic Silica Isolation of Plasma Membrane—Plasma membranes were purified as described (23) with some modifications. Briefly, after treatments, cells were washed twice with ice-cold PBS and twice in ice-cold coating buffer (20 mM MES, 150 mM NaCl, 280 mM sorbitol, pH 5.0–5.5). Cationic silica in a final concentration of 1% was added to the cells in coating buffer for 2 min on ice. Cells were then washed with ice-cold coating buffer to remove excess silica. Sodium polyacrylate (1 mg/ml, pH 6–6.5) was added to the cells in coating buffer and incubated at 4 °C for 2 min. Cells were washed once in ice-cold coating buffer and then washed with modified HES (20 mM HEPES, 250 mM sucrose, 1 mM DTT, 1 mM magnesium acetate, 100 mM potassium acetate, 0.5 mM zinc chloride, pH 7.4) at 4 °C and lysed as described above. Nycodenz (100%) in modified HES buffer was added to the lysate to a final concentration of 50%. The lysate was layered onto 0.5 ml of 70% Nycodenz in modified HES and centrifuged in a swing-out rotor at 25,000 × *g* for 20 min at 4 °C. The supernatant was discarded, and the pellet was resuspended in 0.5 ml of modified HES buffer and centrifuged at 500× *g* for 5 min at 4 °C. The pellet was resuspended in SDS-PAGE sample buffer and heated to 65 °C for 10 min.

siRNA Knockdown of Akt2—3T3-L1 cells at 6–7 days after differentiation were detached using 5 × trypsin/EDTA and washed in DMEM/10% FCS medium containing 4% glycerol. For each reaction, 2 million cells were resuspended in buffer L (Amaxa Cell Line Nucleofector Kit L) containing siRNA at the indicated concentrations. Following electroporation (Amaxa Nucleofector II), cells were resuspended in 2 ml of DMEM/10% FCS and reseeded into 4 × 24-well plates and incubated for 72 h at 37 °C before performing various experiments.

Data Analysis—The data from the experiments were quantified and normalized relative to the response when stimulating 3T3-L1 adipocytes with 100 nM insulin for 20 min. Basal values were subtracted for the fitting of the data. Scaled data from all experiments were combined as a single data set and fitted to a logistic curve,

$$y = a + (b - a)/(1+10\text{^}((\text{LogED}_{50} - x))) \quad \text{(Eq. 1)}$$

using GraphPad Prism, where a is the level at dose zero, which was constrained to zero; b is the level at infinite dose; ED_{50} is the dose at which half-maximal response is observed; and x is the dose. Data are expressed as indicated in the figure legends. p values were calculated by one-way or two-way ANOVA using GraphPad Prism. Three-dimensional surface charts were created in Microsoft Excel where missing values were interpolated.

Computational Prediction Using Cellworks Virtual Adipocyte Platform—Predictive experiments were performed using the Virtual Adipocyte technology built upon an algorithm reported previously (24–26). Briefly, the Cellworks Adipocyte Platform was engineered based on an extensive literature search with each individual process built as a stand-alone module. In the case of inconsistent or unknown enzyme kinetic parameters, a trial-and-error method of optimization was employed to attain physiological outcome. Modules were tested individually for correctness, and predictive values were corroborated with experimental data. The Virtual Adipocyte Platform was stabilized and fixed on control values corresponding to basal condition with 5 mM extracellular glucose concentration. This stabilized system was transitioned into an insulin-stimulated condition. Reduction of Thr-308 Akt1 and/or Akt2 phosphorylation and knockdown of Akt1 and/or Akt2 protein levels were performed.

RESULTS

Inhibition of mTOR Increases Insulin-stimulated Phosphorylation of Akt with Minimal Effect on GLUT4 Translocation—A major goal of this study was to explore the relationship between individual components within the insulin signaling network, with a particular emphasis on Akt. We have previously shown that a small degree of Akt phosphorylation is sufficient to achieve a maximal biological outcome under normal biological circumstances (27, 28). We reasoned that in view of this nonlinearity, changes in the amount of Akt phosphorylation might not be translated into equivalent changes in Akt substrate phosphorylation. To explore this, we first examined the effects of rapamycin on signaling because it has been shown to override a negative feedback loop that attenuates Akt phosphorylation (6, 9, 11). 3T3-L1 adipocytes expressing HA-GLUT4 were exposed to insulin for 10–60 min in the absence or presence of rapamycin. Expression of HA-GLUT4 in 3T3-L1 adipocytes does not alter insulin-dependent activation of the Akt signaling pathway or the -fold response to insulin for glucose uptake (supplemental Fig. S1). Consistent with previous studies (9, 11), rapamycin potentiated insulin-stimulated Akt phosphorylation at both Thr-308 and Ser-473 by ≥2-fold (Fig. 1, *A* and *B*).

To determine whether this effect was mediated via IRS1, we examined the effects of rapamycin on PDGF-stimulated Akt activation in 3T3-L1 adipocytes stably expressing the PDGF receptors because this occurs independently of IRS1 (27). If the mTORC1/S6 kinase negative feedback loop operates at the level of IRS1, one would expect that rapamycin treatment would not have an effect on PDGF-stimulated Akt phosphorylation. However, we observed a significant potentiation of Akt phosphorylation in PDGF-stimulated cells when cells were treated with rapamycin. The extent of increase in Akt phosphorylation was similar to that observed in insulin-stimulated cells

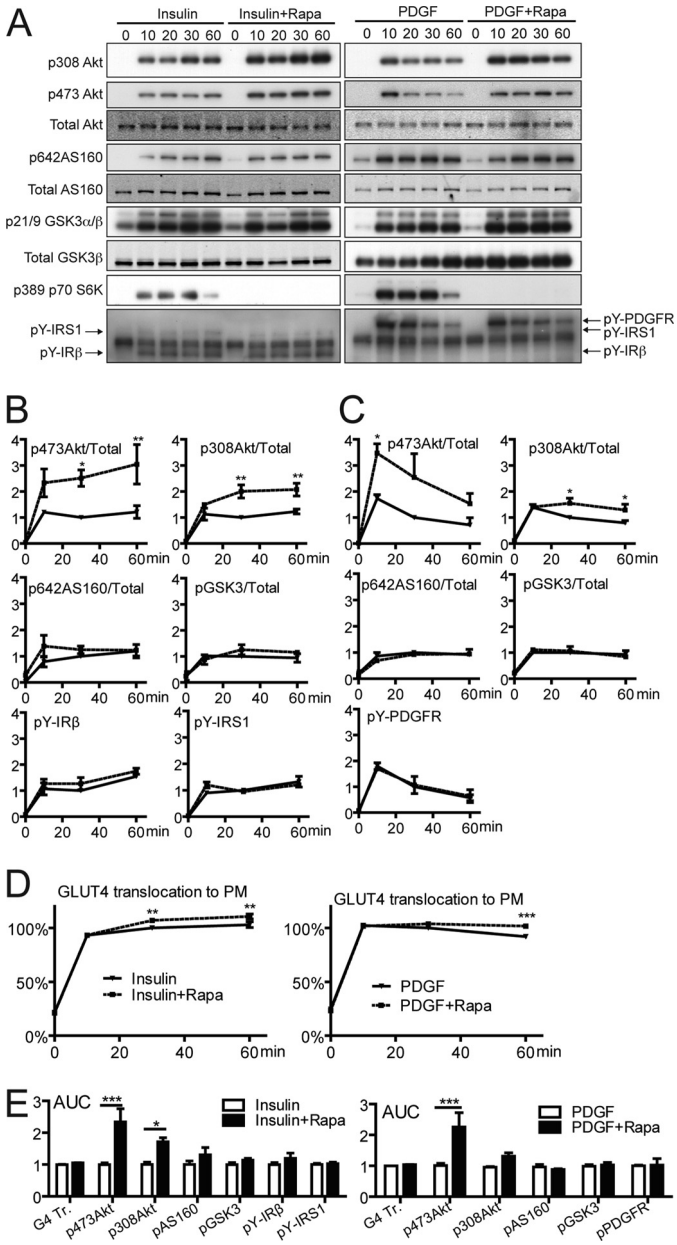

FIGURE 1. **Rapamycin potentiates insulin- and PDGF-stimulated Akt phosphorylation but has no effect on downstream substrates.** Differentiated 3T3-L1 adipocytes or PDGF receptor-expressing 3T3-L1 adipocytes were serum-starved in Krebs-Ringer phosphate buffer for 2 h in the presence or absence of 20 nM rapamycin and stimulated with insulin (200 nM) or PDGF (20 ng/ml) for the indicated time. *A*, total cell lysates immunoblotted with antibodies as described. *B* and *C*, quantification of immunoblots. *D*, GLUT4 translocation measured as described. *E*, integrated area under the curves (*AUC*) of *B* and *C*, respectively. *Error bars* indicate S.E. of three independent experiments. *, $p < 0.05$;**, $p < 0.01$; and ***, $p < 0.001$.

(Fig. 1, *A*–*C*). These data indicate that the rapamycin-sensitive feedback inhibitory pathway that modulates Akt phosphorylation in 3T3-L1 adipocytes is unlikely to be IRS1-dependent.

The potentiation in insulin and PDGF-stimulated Akt activation was not accompanied by a significant change in regulated phosphorylation of Thr-642 AS160 or Ser-9 GSK3β, and there was a relatively minor increase in GLUT4 translocation to the PM in the presence of rapamycin (Fig. 1, *A*–*D*). When the time course curves were integrated, only Akt phosphorylation at Thr-308 and Ser-473 showed a significant increase with rapamycin treatment (Fig. 1*E*). These data indicate that the mTORC1 negative feedback loop operates in adipocytes, and this pathway plays a significant role in attenuating Akt phosphorylation acutely. However, this feedback mechanism does not play a universal role in all Akt-dependent actions.

Acute Inhibition of Akt Phosphorylation Using Small Molecule Inhibitors—To explore the nonlinearity at the Akt node further, we next studied the effect of pharmacological inhibition of Akt with regard to its downstream activity. To modulate the activity of Akt phosphorylation, we made use of isoform-specific inhibitors of Akt (Akti). These inhibitors, Akt1i and Akt2i, specifically inhibit Akt1 and Akt2, respectively, by binding to the PH domain, preventing the interaction of Akt with the PM (20). We have previously documented the effects of these inhibitors on Akt1 and Akt2 activity and have also described a nonspecific effect on the transport activity of the glucose transporter. Therefore, in these studies we focused our analysis on GLUT4 translocation to the PM to avoid this problem (29). To determine the specificity of Akt1i and Akt2i, 3T3-L1 adipocytes were treated with insulin in the presence of various doses of each inhibitor. Akt1 and Akt2 were immunoprecipitated from cell lysates using isoform-specific antibodies (Fig. 2*A*). At the lowest dose (10 μM), each inhibitor exhibited significant specificity with respect to its ability to inhibit phosphorylation of either Akt1 or Akt2, particularly at the Thr-308 site. This was not the case at higher doses (50–100 μM) (Fig. 2*A*). These data indicate that these inhibitors achieve considerable isoform specificity at a concentration of 10 μM.

We next determined the effects of these inhibitors on Akt activity in 3T3-L1 adipocytes. At the lowest dose (10 μM) of each inhibitor, where they exhibited the highest specificity, we observed a more significant inhibitory effect with Akt2i on Akt phosphorylation. Simultaneous addition of both Akt1i and Akt2i at 10 μM resulted in inhibition of Thr-308 and Ser-473 Akt phosphorylation by 85 and 100%, respectively (Fig. 2, *B*–*D*). Despite the magnitude of this effect, there was a relatively modest inhibitory effect on each of the Akt substrates. There was no significant effect of Akt1i alone on any of the substrates measured (Fig. 2, *B* and *E*–*H*). Akt2i alone, at the lowest dose, inhibited insulin-dependent pThr-1462 TSC2, p-Ser9 GSK3, and pThr-642 AS160 by 20–30%. A similar effect was seen for insulin-stimulated GLUT4 translocation (Fig. 2*I*). The combined effects of Akt1i and Akt2i at 10 μM each were not different from that seen with 10 μM Akt2i except in the case of pThr-1462 TSC2 where combined treatment resulted in a much more potent inhibition. At higher drug concentrations we observed substantial inhibition of Akt substrate phosphorylation and GLUT4 translocation either with Akt2i alone or with both in combination. For example, at 50 μM when both drugs were added simultaneously there was almost complete inhibition of pThr-642 AS160, pThr-1462 TSC2, and GLUT4 translocation. This indicates that the inability of the drugs to inhibit these processes at lower doses (10 μM) is not likely due to the activity of an alternate kinase. Looking at the effects of the isoform-specific inhibitors alone, it was clear that Akt1i had little effect on substrate phosphorylation or on GLUT4 translocation at any dose tested. This suggests that even at the highest dose

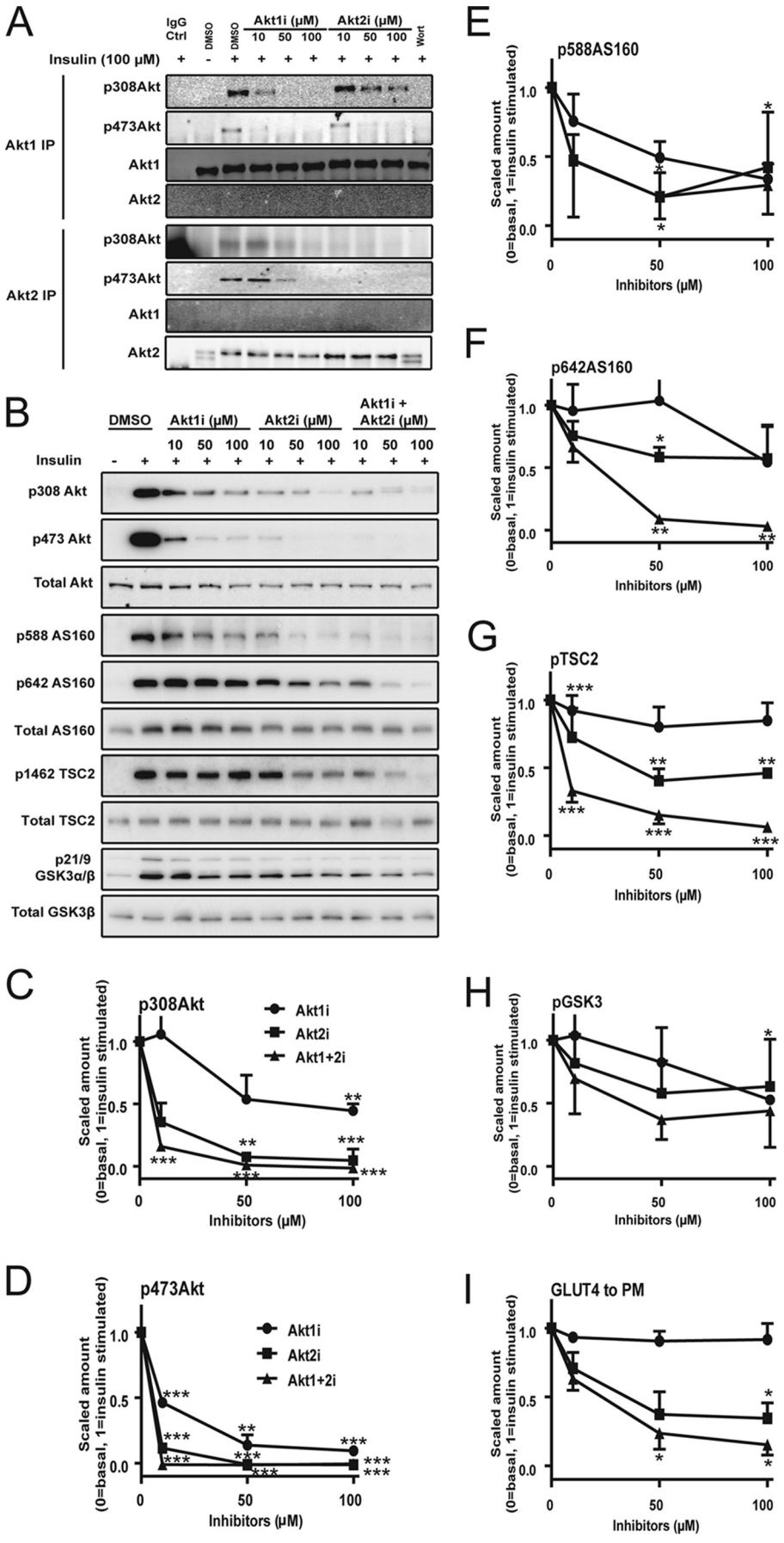
A
IgG Ctrl
DMSO
DMSO
Akt1i (μM)
10 50 100
Akt2i (μM)
10 50 100
Wort
Insulin (100 μM) + - + + + + + + + +
Akt1 IP
p308Akt
p473Akt
Akt1
Akt2
Akt2 IP
p308Akt
p473Akt
Akt1
Akt2
B
DMSO
Akt1i (μM)
Akt2i (μM)
Akt1i + Akt2i (μM)
10 50 100 10 50 100 10 50 100
Insulin - + + + + + + + + + +
p308 Akt
p473 Akt
Total Akt
p588 AS160
p642 AS160
Total AS160
p1462 TSC2
Total TSC2
p21/9 GSK3α/β
Total GSK3β
C
p308Akt
Akt1i
Akt2i
Akt1+2i
Scaled amount (0=basal, 1=insulin stimulated)
Inhibitors (μM)
D
p473Akt
Akt1i
Akt2i
Akt1+2i
Scaled amount (0=basal, 1=insulin stimulated)
Inhibitors (μM)
E
p588AS160
Scaled amount (0=basal, 1=insulin stimulated)
Inhibitors (μM)
F
p642AS160
Scaled amount (0=basal, 1=insulin stimulated)
Inhibitors (μM)
G
pTSC2
Scaled amount (0=basal, 1=insulin stimulated)
Inhibitors (μM)
H
pGSK3
Scaled amount (0=basal, 1=insulin stimulated)
Inhibitors (μM)
I
GLUT4 to PM
Scaled amount (0=basal, 1=insulin stimulated)
Inhibitors (μM)

where there is some cross-reactivity of Akt1i with Akt2 (Fig. 2*A*), there still must be sufficient residual Akt2 activity to sustain normal biological function. This is consistent with previous studies showing a dominant role for the Akt2 isoform in metabolic regulation (30). Despite this, redundancy between Akt1 and Akt2 in terms of most of the downstream actions was evident. This was most clearly evident for the effects of Akt2i on AS160 phosphorylation. At 50 μM, a dose that almost completely blocked Akt2 activation (Fig. 2, *C* and *D*), Akt2i alone had a modest inhibitory effect (42%) on AS160 phosphorylation, and there was no further inhibition even at higher concentrations of the drug (Fig. 2*F*). However, when Akt2i was combined with Akt1i, even at 50 μM, almost complete inhibition of AS160 phosphorylation was evident. AS160 plays an important role in insulin-regulated GLUT4 translocation (31). Based on the present data it seems possible that AS160 may not be the sole determinant of the insulin effect on this process because at 50–100 μM concentrations of Akt2i we observed ~40% inhibition of AS160 phosphorylation at Thr-642 whereas insulin-stimulated GLUT4 translocation was inhibited by >60%. Alternatively, as is the case for Akt, there may also be nonlinearity further down the pathway in which case even modest reductions in AS160 phosphorylation may cause a larger effect on GLUT4 translocation due to the intrinsic threshold at this node.

To confirm these observations using pharmacological inhibitors we used Akt2-specific siRNAs to reduce Akt2 expression in adipocytes (supplemental Fig. S2). Again, a robust reduction in the levels of Akt2 was accompanied by only a modest change in insulin-stimulated phosphorylation of AS160 and S6 (supplemental Fig. S2) and very little if any change in insulin-stimulated GLUT4 translocation (supplemental Fig. S2). These data are consistent with previous reports where reduced Akt2 did not result in similar reductions in downstream insulin actions (30, 32, 33) and the data obtained using the Akt inhibitors.

Minimal Akt Is Sufficient for Downstream Signaling and GLUT4 Translocation—One explanation for the discrepancy between Akt phosphorylation and activity is that, in the cell minimal activation of Akt is required to elicit a robust biological effect. To test this we combined data from all of the studies reported here and examined the relationship between Akt phosphorylation and the other variables (Fig. 3). The relationship between Akt phosphorylation, at both Thr-308 and Ser-473, with GLUT4 translocation, AS160 phosphorylation, GSK3 phosphorylation, and TSC2 phosphorylation was similar, yielding a sigmoidal dose-response curve (Fig. 3, *A* and *B*). The ED_{50} for each of these variables was 0.05–0.22 (Fig. 3*C*). In contrast, AS160 phosphorylation and GLUT4 translocation showed a linear relationship using identical analyses (Fig. 3*D*). This indicates that there is a nonlinear relationship in the absolute level of signal in upstream elements of the pathway. This makes it

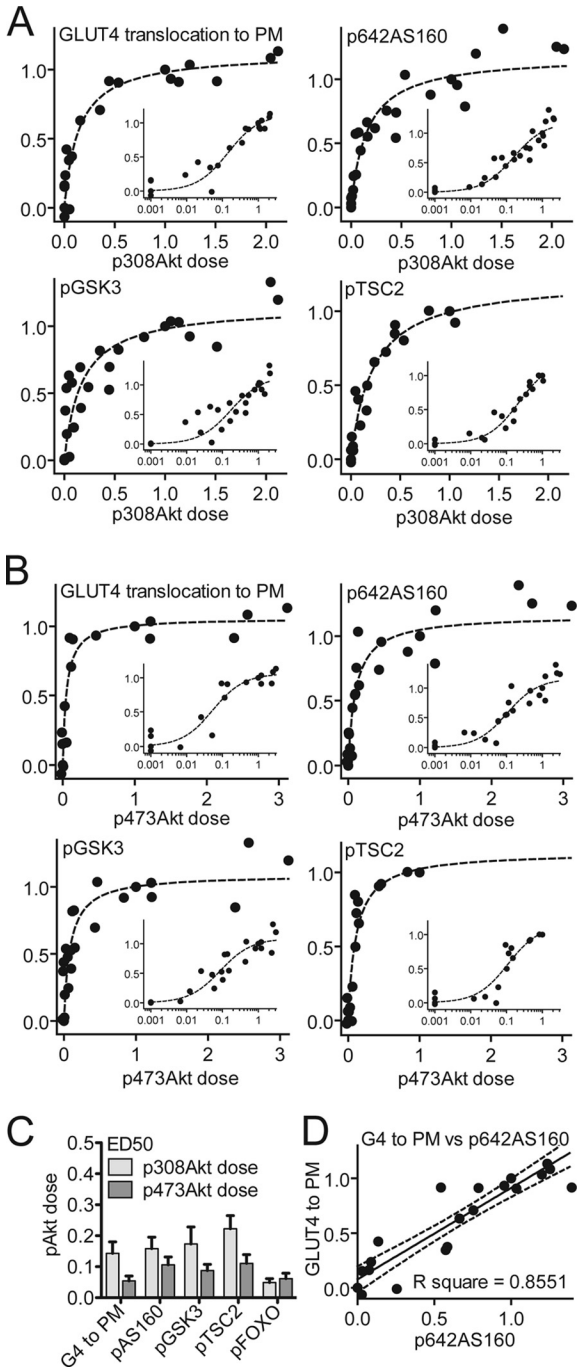

FIGURE 3. **Minimal activation of Akt is required for downstream insulin action.** Data from Figs. 1 and 2 were normalized to the level of either (*A*) Thr-308 or (*B*) Ser-473 Akt phosphorylation that was obtained when 3T3-L1 adipocytes were stimulated with insulin (100 nM) for 20 min. GLUT4 translocation to the PM, pThr-642 AS160, pSer-21/9 GSK3α/β, and pThr-1462 TSC2 was plotted against pThr-308 Akt or pSer-473 Akt on a normal scale and log scale (*inset*). Each data point represents the mean of three independent experiments. *C*, half-maximal dose (ED_{50}) derived from fitting of the data in *A* as described under "Experimental Procedures." *Error bars* indicate S.E. *D*, relationship between GLUT4 translocation and AS160 phosphorylation calculated under identical conditions as a control.

FIGURE 2. **Acute inhibition of Akt using isoform-specific Akt inhibitors.** 3T3-L1 adipocytes were serum-starved in Krebs-Ringer phosphate buffer for 2 h. Cells were treated with either 0.1% dimethyl sulfoxide (*DMSO*) or the indicated dose of Akt1i and/or Akt2i or wortmannin (100 nM, *Wort*) for 30 min prior to exposure to 100 nM insulin for 20 min. *A*, total cell lysates were immunoprecipitated (*IP*) using Akt1 or Akt2 isoform-specific antibodies and immunoblotted with pThr-308 Akt, pSer-473 Akt, Akt1, or Akt2 antibodies. *B*, total cell lysates were immunoblotted with pThr-308 Akt, pSer-473 Akt, total Akt, pSer-588 AS160, pThr-642 AS160, Total AS160, pThr-1462 TSC2, total TSC2, pSer-21/9 GSK3α/β, or GSK3β antibodies. *C–H*, immunoblots were quantified. *I*, HA-GLUT4 translocation was measured as described. *Error bars* indicate S.E. of three independent experiments. *, $p < 0.05$; **, $p < 0.01$; and ***, $p < 0.001$ compared with insulin control.

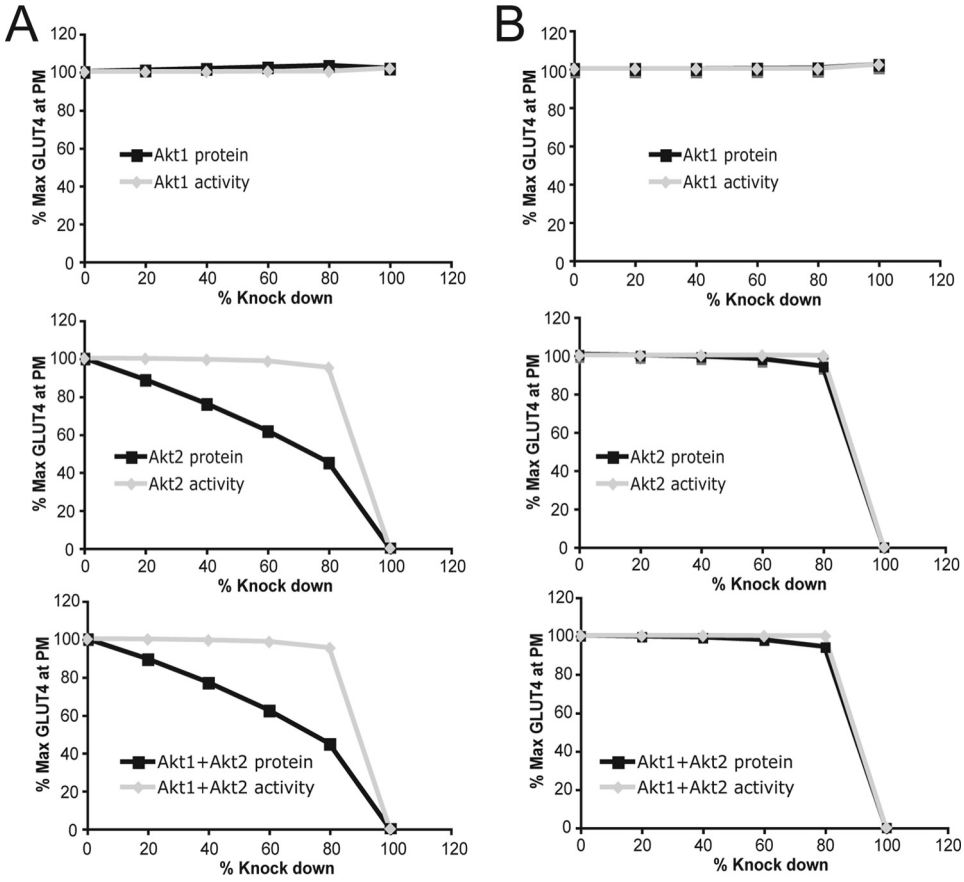

FIGURE 4. **Reduction of Akt protein or phosphorylation level using the Virtual Adipocyte Platform.** *A*, *in silico* effect of reducing the protein level (*black*, *square*) or activity (*gray*, *diamond*) of Akt1, Akt2, or Akt1 and Akt2 on insulin-stimulated GLUT4 translocation to the PM using Akt binding affinity to PI(3,4,5)P3 of 1 μM. *B*, *in silico* effect of reducing Akt1, Akt2, or Akt1 and Akt2 on insulin-stimulated GLUT4 translocation to the PM using Akt binding affinity to PI(3,4,5)P3 of 15 nM.

unlikely that changes in the level of Akt phosphorylation within the upper range of its activity curve (>0.3) will have any significant biological outcome.

In Silico Simulation of Akt Activity and Protein Level on GLUT4 Translocation—We next attempted to simulate these findings using a computational model of the Akt signaling pathway, termed the Virtual Adipocyte Platform. This platform was built, modeled, and validated using previously published data of various signaling events and biological outcomes such as GLUT4 translocation. Initially, the model was unable to replicate the experimental data because the model assumed that Akt associates with the plasma membrane with an affinity of 1 μM (Fig. 4*A*). By increasing the binding affinity of Akt to the PM from 1 μM to 15 nM, approximating the binding affinity of Akt to PI(3,4,5)3P (34), the model yielded a good fit of the data whereby ~10% of Akt2 activity was sufficient to mediate almost 100% of insulin-stimulated GLUT4 translocation to the PM (Fig. 4*B*).

Insulin-stimulated Protein Synthesis Displays Nonlinear Relationship with Akt Activity—We next wanted to establish whether alternate Akt-dependent actions of insulin displayed similar nonlinear behavior. Protein synthesis is also stimulated by insulin, and this is Akt-dependent (35) (supplemental Fig. S3), and its regulation occurs independently of increased glucose transport. The dose-response curve for insulin-stimulated protein synthesis was shifted further to the left compared with GLUT4 translocation, and so maximal activation of protein synthesis was achieved by activation of as little as 2% of the entire Akt pool (Fig. 5, *A* and *B*). Phosphorylation of PRAS40, a regulator of mTORC1 and protein synthesis (36, 37), was less sensitive to insulin compared with protein synthesis *per se* (Fig. 5*A*). These data indicate that the nonlinearity within the insulin signaling pathway is not constrained to GLUT4 translocation.

Nonlinearity at PM—We have shown previously that there is better agreement in the absolute level of Akt phosphorylation at the PM and substrate phosphorylation (28), suggesting that spatial regulation may play a role. To examine this more quantitatively we performed further analyses on the PM fraction isolated from adipocytes. Consistent with our previous studies (28), there was a better correlation between Akt phosphorylation and substrate phosphorylation at the PM, with the ED_{50} for insulin-stimulated pSer-473 Akt at the PM being somewhat lower than that observed in the whole cell lysate (Fig. 6, *A* and *B*). However, this was inadequate to account for the entire discrepancy, and the relationship between phosphorylation of Akt at the PM and its substrates remained sigmoidal (Fig. 6*B*), requiring 19–23% PM Akt phosphorylation for half-maximal substrate phosphorylation (Fig. 6*E*). Interestingly, AS160 phosphorylation at the PM was more sensitive than in the whole cell lysate, raising the possibility that AS160 plays an important functional role at this location (28). To confirm the nonlinearity between PM-localized Akt phosphorylation and its substrates,

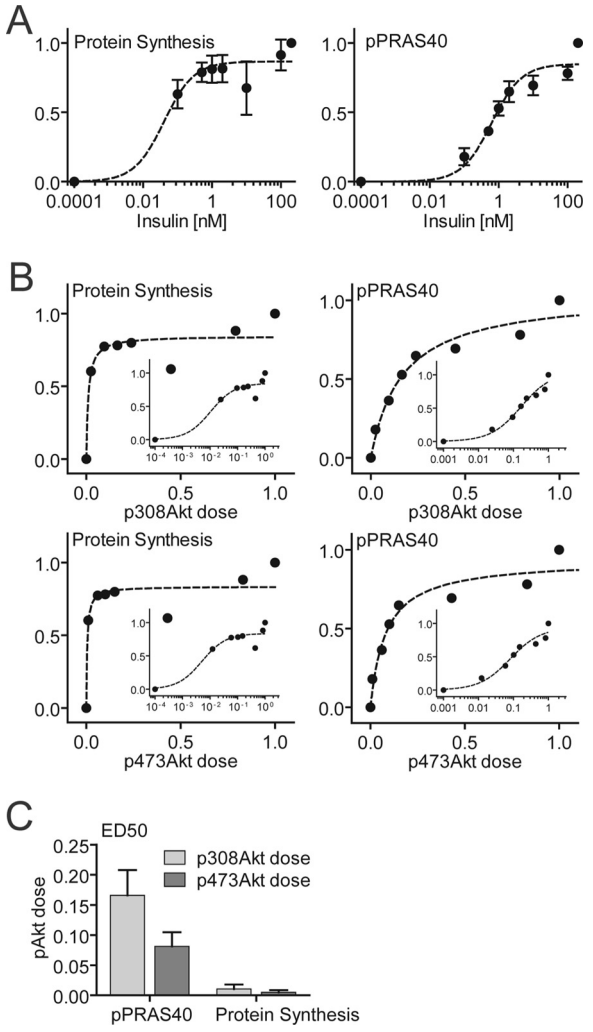

FIGURE 5. **Insulin-mediated protein synthesis displayed a nonlinear relationship with Akt phosphorylation.** 3T3-L1 adipocytes were stimulated with the indicated dose of insulin, and [^{3}H]leucine incorporation into protein was measured as described under "Experimental Procedures." Whole cell lysate was immunoblotted with antibodies specific for pThr-308 Akt, pSer-473 Akt, total Akt, pThr-246 PRAS40, and total PRAS40. *A*, insulin dose-response curve of protein synthesis and pThr-246 PRAS40 phosphorylation. *B*, phosphorylation dose-response curves of pThr-308 Akt or pSer-473 Akt with protein synthesis or pPRAS40. *C*, ED_{50} (pThr-308 Akt dose and pSer-473 Akt dose) derived from fitting of the data. *Error bars* indicate S.E. from three independent experiments.

we analyzed previous data using the rapalog dimerization system (ARIAD) to recruit Akt selectively to the PM for activation (38). The total cell lysate analysis of these experiments represented PM Akt, and consistent with the PM fractionation data, very low levels of rapalog-induced Akt were required for half-maximal substrate phosphorylation (4–9%) (Fig. 6, *D* and *E*).

Akt Substrates Respond to Changes in Rate of Akt Activation—Most of the studies described above have involved measuring the change in the absolute level of phosphorylation at a specific time point. We next wanted to examine the possibility that Akt substrates may better respond to changes in the rate of Akt phosphorylation. By examining the time course of phosphorylation at two separate insulin doses we made the following observations. First, overall there was a strong correlation between the initial rate of change in phosphorylation in all parameters measured (Fig. 7, *A* and *B*). Second, there was a dose-dependent increase in the initial rate of phosphorylation for Akt, AS160, PRAS40, and GSK3 but not for FoxO1 (Fig. 7, *A* and *B*). These data highlight the rate of change of Akt phosphorylation as a key parameter in signal transmission. When dose- and time-dependent phosphorylation were plotted together in a three-dimensional surface chart, it was obvious that the three-dimensional surface of p473Akt differed from both pAS160 as well as pFoxO1 (Fig. 7*C*), further emphasizing the demultiplexing capacity at the level of Akt.

DISCUSSION

Akt is a major regulatory node for many essential biological processes. A number of feedback intermediates have been described that modulate Akt signaling (9, 12, 39). We have previously found that a relatively small amount of Akt phosphorylation is required to elicit robust outputs (27, 28, 40). Hence, changes in Akt phosphorylation do not translate into equivalent changes downstream. In the current study we provide evidence that Akt displays switch-like and/or sensitivity amplification behavior. Moreover, there is heterogeneity in the engagement of Akt with its different substrates in terms of dose and kinetic behavior, raising the possibility of demultiplexing within the pathway.

A range of possibilities could explain the relationship between Akt and its downstream substrates. This includes spatial regulation of components in the pathway or the existence of feedback or feedforward loops as has been documented for other signaling systems (41). We have attempted to interrogate the role of spatial regulation in the present studies, and although there did seem to be a closer correspondence between Akt and substrate phosphorylation at the PM this was still insufficient to explain the lack of concordance between Akt phosphorylation and that of its substrates. The PM is a heterogeneous organelle, however being comprised of raft and non-raft domains. It has also been proposed that AS160 is phosphorylated when attached to intracellular GLUT4 vesicles (21, 31). Therefore, a more rigorous analysis of the subcellular distribution of the components in the insulin signaling pathway needs to be undertaken to determine the contribution of spatial regulation to the quantitative relationship between each of the components in the pathway.

Experimental investigation of feedback pathways in signal transduction is complicated. A limitation of the present studies is that all studies were performed on cell populations, and so the outputs potentially represent the average of many different responses in individual cells. Regardless, a notable feature of the outputs measured is that in the adipocyte there was little evidence for adaptive behavior as would be the case if the pathway were dominated by negative feedback loops. For instance, the insulin addition was accompanied by a rapid rise to a new steady state, and this was maintained as long as insulin was present in the medium. There was evidence for attenuation of Akt308 phosphorylation at low insulin doses (Fig. 7*A*), but this did not translate into changes downstream in the pathway.

One notable feature was the switch like behavior at Akt. The relationship between Akt phosphorylation and all other parameters measured was sigmoidal with a steep response at around the physiological insulin concentration whereas the relation-

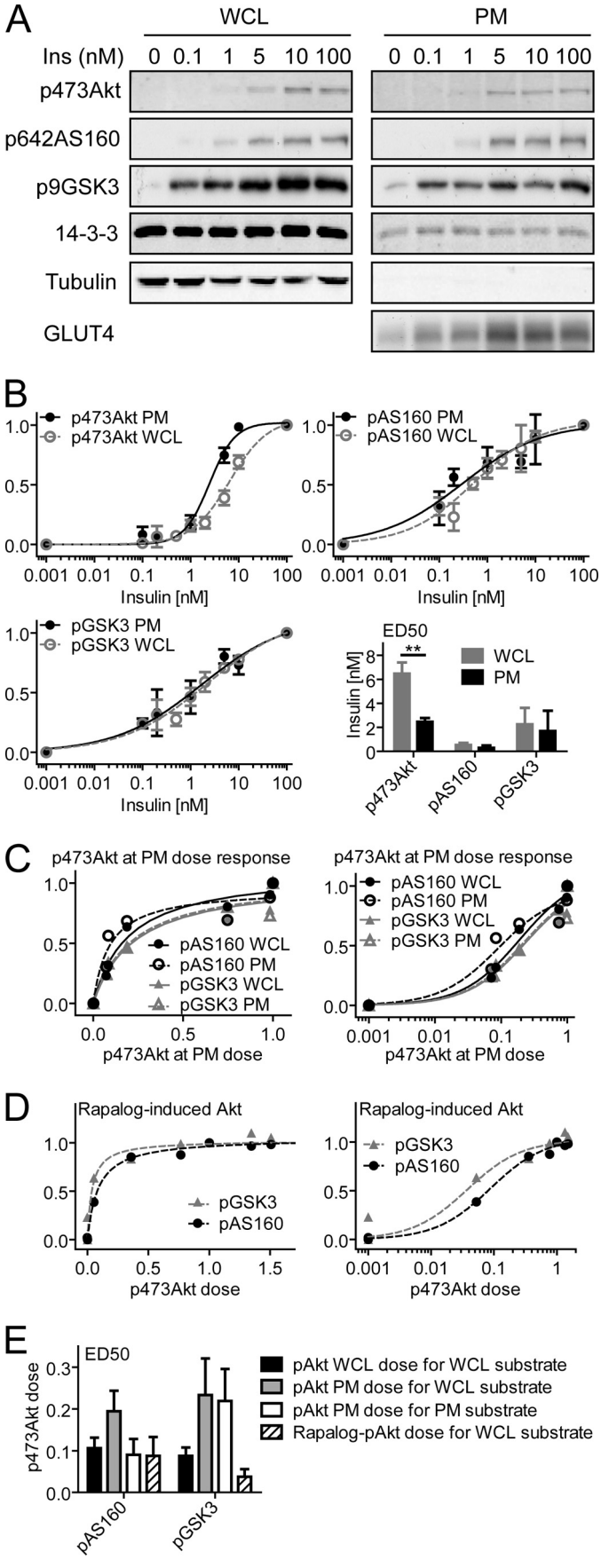

ship between Akt substrate AS160, and its presumed end point GLUT4 translocation was linear. As noted by Koshland *et al.* (42) sigmoidal behavior is characteristic of sensitivity amplification steps. In this case a 10% change in the input (Akt phosphorylation) gives rise to a 50% change in the output (see Fig. 3). This indicates that Akt is highly sensitive, providing the basis for amplification. This behavior is intriguing because contrary to early expectations there is little evidence for amplification in proximal elements of the pathway, and so Akt may represent one of the major amplification steps in the pathway.

It is well established that mTOR forms part of a negative feedback loop within the insulin signaling pathway, and multiple targets including IRS1 and Rictor have been suggested (8–12, 39). Our studies show that this loop exists in adipocytes but that IRS1 may not be the major target of feedback regulation. Our data are consistent with the recently described inhibitory effect of mTOR/S6K on Rictor, a subunit of mTORC2 that phosphorylates Akt on Ser-473 (12). Another feature of the feedback loop is that it does not appear to have a major impact on signaling under conditions of robust activation. This is not surprising as small amplitude negative feedback loops probably play a more important role in stabilizing signaling under basal conditions (41). It is conceivable then that the mTOR negative feedback loop combined with the amplification step at Akt play a key role in filtering out noise that might influence the system under nonstimulated conditions. It is likely that we have overlooked the impact of this parameter in the present study because we have used an artificial basal condition of zero insulin. *In vivo*, the basal condition varies throughout the day, particularly because insulin is secreted in an oscillatory manner with a period of 10–15 min (43) even under fasting conditions.

We also noted a lack of concordance in behavior of components downstream of Akt. For example, FoxO1 phosphorylation was more sensitive to insulin, shown by its low ED_{50} for pAkt, than the phosphorylation of other substrates (Fig. 3*C*), whereas protein synthesis was more sensitive than GLUT4 translocation (Figs. 3*C* and 5*C*). This suggests that the input signal, in this case insulin, can be split into multiple discrete outputs as the signal filters down the pathway. This demultiplexing characteristic is potentially important as it raises the possibility that it might be possible to target specific outputs without perturbing the activity of others. So in the context of a cancer cell it would be desirable to design a drug to cancel out the antiapoptotic function of Akt while preserving other activities of the pathway.

A technical implication of these studies is that caution should be taken in equating levels of Akt phosphorylation with Akt

FIGURE 6. **Phosphorylation of Akt at the PM is more sensitive to insulin but is still disconnected from Akt substrate phosphorylation.** *A*, differentiated 3T3-L1 adipocytes stimulated for 30 min with the indicated dose of insulin. Subsequently, the PM fraction was isolated, and both PM fraction and whole cell lysate (*WCL*) were immunoblotted with antibodies specific for pSer-473 Akt, total Akt, pThr-642 AS160, total AS160, pSer-21/9 GSK3α/β, total GSK3β, tubulin, and 14-3-3. *B*, quantification of immunoblots in *A*. ED_{50} (insulin dose) was derived from fitting of the data. *Error bars* indicate S.E. from three independent experiments. *C*, phosphorylation dose-response curves of pSer-473 Akt with pThr-642 AS160 and pSer-9 GSK3β in the whole cell lysate or at the PM. *D*, quantification of rapalog-induced Akt data published in Ref. 38. *E*, ED_{50} (pSer-473 Akt dose) derived from fitting of the data in *C* and *D*. *Error bars* indicate S.E.

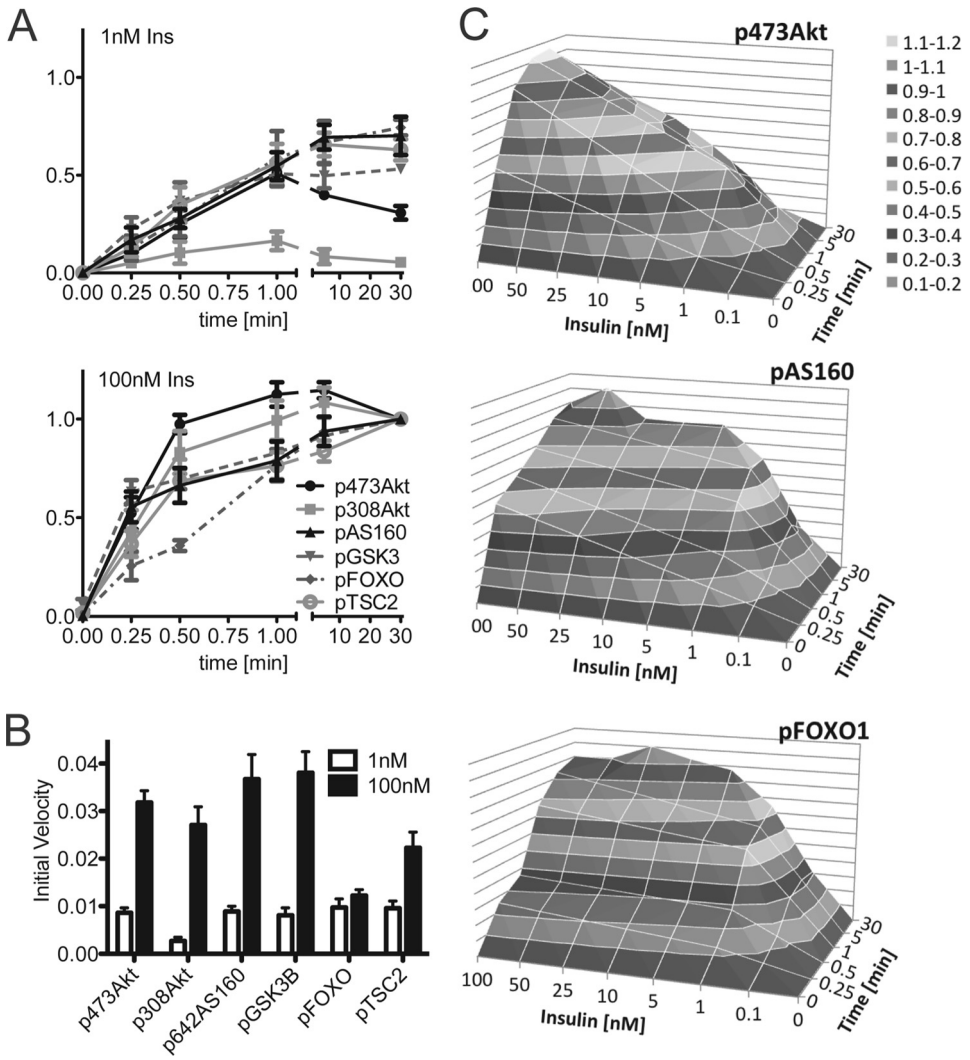

FIGURE 7. **Initial rate of phosphorylation of Akt and its substrates is highly correlated.** *A*, 3T3-L1 adipocytes were stimulated with 1 or 100 nM insulin for the indicated time, and total cell lysates were immunoblotted with a range of antibodies as indicated. Immunoblots were quantified and normalized to the 30 min 100 nM insulin value. *Error bars* indicate S.E. of three independent experiments. *B*, initial rate was calculated by fitting a linear regression to the initial, linear time points. *Error bars* indicate the S.E. *C*, three-dimensional surface chart was created using the time course data shown in *A* (*depth axis*) and the dose-response data published in Ref. 28 (*horizontal axis*) with the missing data points interpolated. The *vertical axis* represents the response in gray scale color code as shown in the legend.

activity particularly at the higher end of the response range. It is clear from these studies that the PI3K/Akt pathway displays a similar degree of complexity to other signaling pathways (44). This comprises sensitization amplification, demultiplexing capacity, and positive and negative feedback. This is likely encoded by a combination of covalent and allosteric regulatory mechanisms. Although our studies have focused on the forward reactions in the pathway, the opposing reactions regulated by phosphatases are likely to be equally important. Finally, because Akt substrates are found in discrete cellular locations, spatial aspects also must not be overlooked.

Acknowledgments—We thank Dr. Adelle Coster (UNSW) for assistance with data analysis and advice, Merck for providing the Akt1-specific and Akt2-specific inhibitors, and Dr. James Cantley (Garvan Institute of Medical Research) for critically reading the manuscript.

REFERENCES

1. Alessi, D. R., and Downes, C. P. (1998) The role of PI 3-kinase in insulin action. *Biochim. Biophys. Acta* **1436,** 151–164
2. Whiteman, E. L., Cho, H., and Birnbaum, M. J. (2002) Role of Akt/protein kinase B in metabolism. *Trends Endocrinol. Metab.* **13,** 444–451
3. Alessi, D. R., Andjelkovic, M., Caudwell, B., Cron, P., Morrice, N., Cohen, P., and Hemmings, B. A. (1996) Mechanism of activation of protein kinase B by insulin and IGF-1. *EMBO J.* **15,** 6541–6551
4. Sarbassov, D. D., Guertin, D. A., Ali, S. M., and Sabatini, D. M. (2005) Phosphorylation and regulation of Akt/PKB by the rictor-mTOR complex. *Science* **307,** 1098–1101
5. Manning, B. D., and Cantley, L. C. (2007) AKT/PKB signaling: navigating downstream. *Cell* **129,** 1261–1274
6. Huang, J., and Manning, B. D. (2009) A complex interplay between Akt, TSC2, and the two mTOR complexes. *Biochem. Soc. Trans.* **37,** 217–222
7. Kahn, C. R. (1978) Insulin resistance, insulin insensitivity, and insulin unresponsiveness: a necessary distinction. *Metabolism* **27,** 1893–1902
8. Takano, A., Usui, I., Haruta, T., Kawahara, J., Uno, T., Iwata, M., and Kobayashi, M. (2001) Mammalian target of rapamycin pathway regulates insulin signaling via subcellular redistribution of insulin receptor sub-

strate 1 and integrates nutritional signals and metabolic signals of insulin. *Mol. Cell. Biol.* **21,** 5050–5062
9. Tremblay, F., Gagnon, A., Veilleux, A., Sorisky, A., and Marette, A. (2005) Activation of the mammalian target of rapamycin pathway acutely inhibits insulin signaling to Akt and glucose transport in 3T3-L1 and human adipocytes. *Endocrinology* **146,** 1328–1337
10. Tzatsos, A., and Kandror, K. V. (2006) Nutrients suppress phosphatidylinositol 3-kinase/Akt signaling via raptor-dependent mTOR-mediated insulin receptor substrate 1 phosphorylation. *Mol. Cell. Biol.* **26,** 63–76
11. Haruta, T., Uno, T., Kawahara, J., Takano, A., Egawa, K., Sharma, P. M., Olefsky, J. M., and Kobayashi, M. (2000) A rapamycin-sensitive pathway down-regulates insulin signaling via phosphorylation and proteasomal degradation of insulin receptor substrate-1. *Mol. Endocrinol.* **14,** 783–794
12. Dibble, C. C., Asara, J. M., and Manning, B. D. (2009) Characterization of Rictor phosphorylation sites reveals direct regulation of mTOR complex 2 by S6K1. *Mol. Cell. Biol.* **29,** 5657–5670
13. Gonzalez, E., and McGraw, T. E. (2009) The Akt kinases: isoform specificity in metabolism and cancer. *Cell Cycle* **8,** 2502–2508
14. Gonzalez, E., and McGraw, T. E. (2009) Insulin-modulated Akt subcellular localization determines Akt isoform-specific signaling. *Proc. Natl. Acad. Sci. U.S.A.* **106,** 7004–7009
15. Dummler, B., Tschopp, O., Hynx, D., Yang, Z. Z., Dirnhofer, S., and Hemmings, B. A. (2006) Life with a single isoform of Akt: mice lacking Akt2 and Akt3 are viable but display impaired glucose homeostasis and growth deficiencies. *Mol. Cell. Biol.* **26,** 8042–8051
16. Knight, Z. A., Gonzalez, B., Feldman, M. E., Zunder, E. R., Goldenberg, D. D., Williams, O., Loewith, R., Stokoe, D., Balla, A., Toth, B., Balla, T., Weiss, W. A., Williams, R. L., and Shokat, K. M. (2006) A pharmacological map of the PI3K family defines a role for p110α in insulin signaling. *Cell* **125,** 733–747
17. Foukas, L. C., Claret, M., Pearce, W., Okkenhaug, K., Meek, S., Peskett, E., Sancho, S., Smith, A. J., Withers, D. J., and Vanhaesebroeck, B. (2006) Critical role for the p110α phosphoinositide-3-OH kinase in growth and metabolic regulation. *Nature* **441,** 366–370
18. Nakae, J., Kitamura, T., Kitamura, Y., Biggs, W. H., 3rd, Arden, K. C., and Accili, D. (2003) The forkhead transcription factor FoxO1 regulates adipocyte differentiation. *Dev. Cell* **4,** 119–129
19. Tellam, J. T., Macaulay, S. L., McIntosh, S., Hewish, D. R., Ward, C. W., and James, D. E. (1997) Characterization of Munc-18c and syntaxin-4 in 3T3-L1 adipocytes: putative role in insulin-dependent movement of GLUT-4. *J. Biol. Chem.* **272,** 6179–6186
20. DeFeo-Jones, D., Barnett, S. F., Fu, S., Hancock, P. J., Haskell, K. M., Leander, K. R., McAvoy, E., Robinson, R. G., Duggan, M. E., Lindsley, C. W., Zhao, Z., Huber, H. E., and Jones, R. E. (2005) Tumor cell sensitization to apoptotic stimuli by selective inhibition of specific Akt/PKB family members. *Mol. Cancer Ther.* **4,** 271–279
21. Larance, M., Ramm, G., Stöckli, J., van Dam, E. M., Winata, S., Wasinger, V., Simpson, F., Graham, M., Junutula, J. R., Guilhaus, M., and James, D. E. (2005) Characterization of the role of the Rab GTPase-activating protein AS160 in insulin-regulated GLUT4 trafficking. *J. Biol. Chem.* **280,** 37803–37813
22. Govers, R., Coster, A. C., and James, D. E. (2004) Insulin increases cell surface GLUT4 levels by dose dependently discharging GLUT4 into a cell surface recycling pathway. *Mol. Cell. Biol.* **24,** 6456–6466
23. Chaney, L. K., and Jacobson, B. S. (1983) Coating cells with colloidal silica for high yield isolation of plasma membrane sheets and identification of transmembrane proteins. *J. Biol. Chem.* **258,** 10062–10072
24. Vali, S., Pallavi, R., Kapoor, S., and Tatu, U. (2010) Virtual prototyping study shows increased ATPase activity of Hsp90 to be the key determinant of cancer phenotype. *Syst. Synth. Biol.* **4,** 25–33
25. Cirstea, D., Hideshima, T., Rodig, S., Santo, L., Pozzi, S., Vallet, S., Ikeda, H., Perrone, G., Gorgun, G., Patel, K., Desai, N., Sportelli, P., Kapoor, S., Vali, S., Mukherjee, S., Munshi, N. C., Anderson, K. C., and Raje, N. (2010) Dual inhibition of Akt/mammalian target of rapamycin pathway by nanoparticle albumin-bound rapamycin and perifosine induces antitumor activity in multiple myeloma. *Mol. Cancer Ther.* **9,** 963–975
26. Shanmugam, M. K., Rajendran, P., Li, F., Nema, T., Vali, S., Abbasi, T., Kapoor, S., Sharma, A., Kumar, A. P., Ho, P. C., Hui, K. M., and Sethi, G. (2011) Ursolic acid inhibits multiple cell survival pathways leading to suppression of growth of prostate cancer xenograft in nude mice. *J. Mol. Med.* **89,** 713–727
27. Hoehn, K. L., Hohnen-Behrens, C., Cederberg, A., Wu, L. E., Turner, N., Yuasa, T., Ebina, Y., and James, D. E. (2008) IRS1-independent defects define major nodes of insulin resistance. *Cell Metab.* **7,** 421–433
28. Ng, Y., Ramm, G., Burchfield, J. G., Coster, A. C., Stöckli, J., and James, D. E. (2010) Cluster analysis of insulin action in adipocytes reveals a key role for Akt at the plasma membrane. *J. Biol. Chem.* **285,** 2245–2257
29. Tan, S. X., Ng, Y., and James, D. E. (2010) Akt inhibitors reduce glucose uptake independently of their effects on Akt. *Biochem. J.* **432,** 191–197
30. Cho, H., Mu, J., Kim, J. K., Thorvaldsen, J. L., Chu, Q., Crenshaw, E. B., 3rd, Kaestner, K. H., Bartolomei, M. S., Shulman, G. I., and Birnbaum, M. J. (2001) Insulin resistance and a diabetes mellitus-like syndrome in mice lacking the protein kinase Akt2 (PKBβ). *Science* **292,** 1728–1731
31. Sano, H., Kane, S., Sano, E., Mîinea, C. P., Asara, J. M., Lane, W. S., Garner, C. W., and Lienhard, G. E. (2003) Insulin-stimulated phosphorylation of a Rab GTPase-activating protein regulates GLUT4 translocation. *J. Biol. Chem.* **278,** 14599–14602
32. Katome, T., Obata, T., Matsushima, R., Masuyama, N., Cantley, L. C., Gotoh, Y., Kishi, K., Shiota, H., and Ebina, Y. (2003) Use of RNA interference-mediated gene silencing and adenoviral overexpression to elucidate the roles of AKT/protein kinase B isoforms in insulin actions. *J. Biol. Chem.* **278,** 28312–28323
33. Jiang, Z. Y., Zhou, Q. L., Coleman, K. A., Chouinard, M., Boese, Q., and Czech, M. P. (2003) Insulin signaling through Akt/protein kinase B analyzed by small interfering RNA-mediated gene silencing. *Proc. Natl. Acad. Sci. U.S.A.* **100,** 7569–7574
34. Currie, R. A., Walker, K. S., Gray, A., Deak, M., Casamayor, A., Downes, C. P., Cohen, P., Alessi, D. R., and Lucocq, J. (1999) Role of phosphatidylinositol 3,4,5-trisphosphate in regulating the activity and localization of 3-phosphoinositide-dependent protein kinase-1. *Biochem. J.* **337,** 575–583
35. Tan, S., Ng, Y., and James, D. E. (2011) Next-generation Akt inhibitors provide greater specificity: effects on glucose metabolism in adipocytes. *Biochem. J.* **435,** 539–544
36. Wang, L., Harris, T. E., Roth, R. A., and Lawrence, J. C., Jr. (2007) PRAS40 regulates mTORC1 kinase activity by functioning as a direct inhibitor of substrate binding. *J. Biol. Chem.* **282,** 20036–20044
37. Kazi, A. A., and Lang, C. H. (2010) PRAS40 regulates protein synthesis and cell cycle in C2C12 myoblasts. *Mol. Med.* **16,** 359–371
38. Ng, Y., Ramm, G., Lopez, J. A., and James, D. E. (2008) Rapid activation of Akt2 is sufficient to stimulate GLUT4 translocation in 3T3-L1 adipocytes. *Cell Metab.* **7,** 348–356
39. Rice, K. M., Turnbow, M. A., and Garner, C. W. (1993) Insulin stimulates the degradation of IRS-1 in 3T3-L1 adipocytes. *Biochem. Biophys. Res. Commun.* **190,** 961–967
40. Whitehead, J. P., Molero, J. C., Clark, S., Martin, S., Meneilly, G., and James, D. E. (2001) The role of Ca^{2+} in insulin-stimulated glucose transport in 3T3-L1 cells. *J. Biol. Chem.* **276,** 27816–27824
41. Brandman, O., Ferrell, J. E., Jr., Li, R., and Meyer, T. (2005) Interlinked fast and slow positive feedback loops drive reliable cell decisions. *Science* **310,** 496–498
42. Koshland, D. E., Jr., Goldbeter, A., and Stock, J. B. (1982) Amplification and adaptation in regulatory and sensory systems. *Science* **217,** 220–225
43. O'Rahilly, S., Turner, R. C., and Matthews, D. R. (1988) Impaired pulsatile secretion of insulin in relatives of patients with non-insulin-dependent diabetes. *N. Engl. J. Med.* **318,** 1225–1230
44. Mak, D. O., McBride, S., and Foskett, J. K. (1998) Inositol 1,4,5-trisphosphate [correction of tris-phosphate] activation of inositol trisphosphate [correction of tris-phosphate] receptor Ca^{2+} channel by ligand tuning of Ca^{2+} inhibition. *Proc. Natl. Acad. Sci. U.S.A.* **95,** 15821–15825